Appendix A: Counter flow atomizer: Effect of the area ratio of the outlet orifice and the inlet air canal

Karolína Smutková[1,*], Milan Malý[1], *Ondřej Cejpek*[1], and *Jan Jedelský*[1]

[1]Brno University of Technology, Faculty of Mechanical Engineering, Czech Republic

Abstract. The need to reduce the energy demand of processes also creates pressure to make atomizers more efficient. A promising development path could be counterflow atomizers (CFA). Initial results suggest that CFA is capable of the same quality of atomization but using half the air mass flow rate compared to conventional twin-fluids atomizers when operated at identical inlet pressure. This means half the energy requirements with the same efficiency. This atomizer also shows a great promise in the atomization of highly viscous substances such as waste-based fuels and biomass oils.

In CFA, the air expands twice; first, at the discharge from the air inlet canal into the mixing tube, and second, at the discharge from the atomizer to the surrounding atmosphere. Therefore, one of the main control parameters is the area ratio of the exit orifice and the air inlet canal. This study experimentally investigates the effect of this ratio on the spray quality for two different CFA atomizers using Phase Doppler Anemometry (PDA), which provides the velocity and size of individual droplet in the spray. The atomizers were operated at the air inlet pressure of 100 and 200 kPa and gas-to-liquid mass (*GLR*) ratios of 5, 10 and 20%.

The effect of the double expansion can be well observed in the pressure differences between the air inlet and the pressure inside the mixing tube. The length of the air counterflow insert had a significant effect on the atomizer performance. For the shorter counterflow channel, a minimal effect on flow was observed; this atomizer behaved like a conventional twin-fluid atomizer and all expansions occurred downstream of the exit orifice. The longer counterflow canal changed the internal expansion ratios, larger droplets, wider spray and higher discharge coefficients (C_d) were obtained.

1 Introduction

At the present time, when the pressure for low energy consumption and renewability, which is often associated with higher viscosity in liquids, is the most intense in the history of mankind, the counterflow atomizers seem to be one of the promising paths for development. For CFA, it is interesting to note that there are only brief references to them from the 20th century and only few recent articles.

Hoxie et al. [1] compared the characteristics of CFA against commercially available internal mixing air assist atomizers. They used water and glycol, and exit diameters close to ours. They designed the CF atomizer in Fig. 1 where the geometry is without our more significant mixing area. Drops were imaged using a standard shadowgraph technique utilizing a pulsed laser as a light source to provide a diffuse background.

The CFA with a larger exit orifice showed large differences in performance at the lowest pressure tested compared to the commercial CA in terms of sensitivity to the change in *GLR*, the D_{32} dropped by 35% for a change of 10% in *GLR*. For the more viscous medium, the CFA produced a narrower droplet distribution. Compared to the water measurements, the drop in GLR was accompanied by a drop in ID_{32}.

The most significant outcome of their study is that, even for large flow rates, D_{32} values remain at or less than 20 microns, despite using *GLR* values less than 20%. The high sensitivity of the D_{32} to *GLR* suggests that much smaller values of D_{32} may be attained without

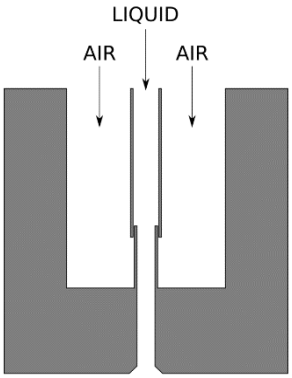

Fig. 1. A. Hoxie et al - CF atomizer

significant increases in *GLR*. Efficiency over a COM atomizer is increased by nearly 100%. The authors describe this performance trend as increasing with increasing viscosity, but they do not know the reason for this phenomenon.

The most significant outcome of their study is that, even for large flow rates, D_{32} values remain at or less than 20 microns, despite using *GLR* values less than 20%. The high sensitivity of the D_{32} to *GLR* suggests that much smaller values of D_{32} may be attained without significant increases in *GLR*. Efficiency over a COM atomizer is increased by nearly 100%. The authors describe this performance trend as increasing with increasing viscosity, but they do not know the reason for this phenomenon.

Rangarajan et al. [2] also studied CFA that they compared to the 'flow-blurring' (FB) atomizer studied by other investigators for four test liquids of viscosity

* Corresponding author: 200171@vutbr.cz

ranging from 1 to 133.5 mPa.s. Both atomizers are shown in Figure 2. Detailed measurements of droplet size distributions were carried out using laser shadowgraphy, along with high-speed flow visualization. In their study, the two-dimensional (2D) simulations are conducted by the "compressible Multiphase Inter Foam" solver in the OpenFOAM-6 toolbox. They used water, propylene glycol and glycerol/water (85%-15% v/v). For a fixed q_{liquid} 60 ml/min, the *GLR* was between 25 and 100%.

Regarding the dependence of D_{32} on *GLR*, they obtained similar results to [1]. The CFA produces a spray whose characteristics are relatively insensitive to fluid viscosity over the range studied, for gas-liquid mass flow ratios between 0.25 and 1. They found that the CFA generates a spray with D_{32} that are very weakly sensitive to the changes of viscosity over two orders of magnitude. This is consistent with the hypothesis mentioned in their paper that the counterflowing velocity and density profiles establish a flow with high levels of turbulent stresses. The mixing process appears essentially incompressible, with a scaling that depends primarily on the volumetric flow rates of atomizing air.

High-fidelity simulations suggest that the primary mechanism responsible for spray formation is a Kelvin-Helmoltz-type instability of the liquid jet inside the nozzle, rendering it insensitive to liquid viscosity.

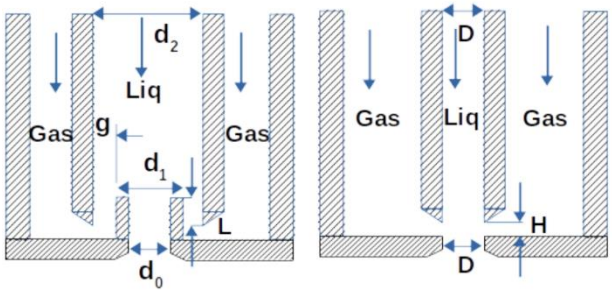

Figure 2. Left - CF atomizer as tested in [2], right – FB atomizer

In this study, it was focused on a part of the internal geometry of these atomizers, namely the ratio of the areas of the outlet orifice and the air inlet canal, as this is a relatively unexplored issue. As can be seen in Fig. 3, the liquid and gas supply to these atomizers is parallel, the counterflow effect is caused by the internal geometry, more precisely by the air supply channel to the mixing chamber. It was been investigated the dependence of Integral Sauter Mean Diameter (*ISMD; ID*$_{32}$), Spray Cone Angle (*SCA*) and C_d on *GLR* at pressures (p_1) 100 and (p_2) 200 kPa for 2 nozzles differing in air inlet channel length and outlet diameters.

2 Experimental setup

The experimental data included in this paper were acquired using a specially designed test bench in the Spray laboratory at Brno University of Technology. All experiments were performed at room temperature (22 °C). The following paragraphs describe the equipment and instrumentation used and include a short discussion over the atomizers and PDA system.

2.1 Atomizers

For this paper, two CFAs with slightly different geometries were used; their design was based on the expertise of articles dealing with similar issues [1, 2].

For simplicity, markings reflecting the atomizer type and outlet diameter have been introduced:

D**x.y**_CF**z**

where **x.y** is a diameter of exit orifice [mm] and **z** = 1 → shorter CF canal; = 2 → longer CF canal

It was focused on the ratio of the areas of the exit orifice and the air inlet canal. These affect the double expansion ratio, which implies the atomization quality and energy requirements. It was hypothesized that, with the lengthening of the counterflow canal, more of the expansion would take place in the mixing chamber, thus achieving better spray parameters compared to conventional atomizers. It was also predicted that the droplet size would increase with the exit orifice.

As seen in Fig. 3. below, our CFA has one axial liquid inlet in the central axis and six axial symmetrically placed air inlets leading into the annulus. The turnover of the jet is caused by the central canal.

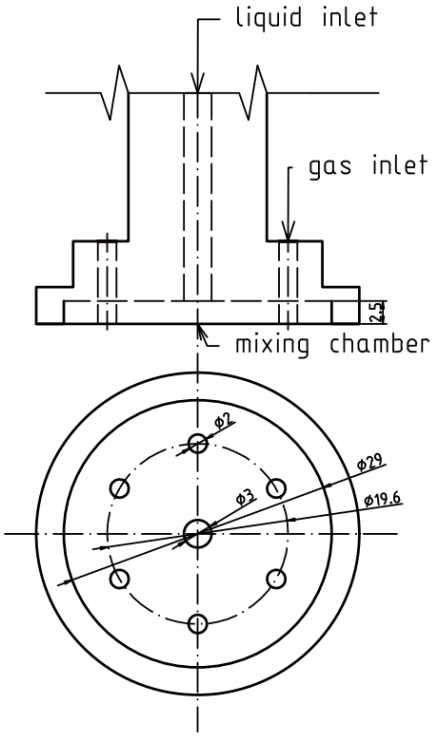

Fig. 3. Body of the counterflow atomizer

The atomizers differed in the diameter of the outlet opening and the length of the counterflow channel (Fig. 4.). The nozzle with the shorter counterflow canal was manufactured with 1.0, 1.5, and 2 mm exit orifice diameter, while the nozzle with the longer counterflow canal was manufactured with 1.4, 1.7, and 2.1 mm. All the variants were measured at *GLR* of 5, 10 and 20% and air pressures of 100 and 200 kPa.

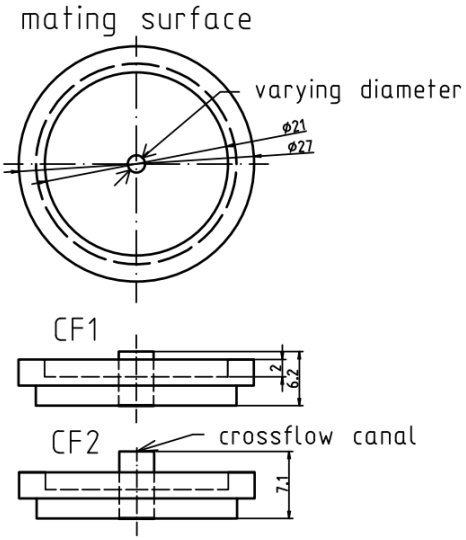

Fig. 4. Exit orifice plate

2.2 PDA system

The size and velocity of the spray droplets were probed using a two-component fibre-based commercial PDA (Dantec Dynamics A/S Skovlunde, DK), Fig. 5 The PDA is able to acquire the axial, radial or tangential velocity components in the coincidence mode along with the simultaneous drop sizes; in this case, only 1D measurement was used as the radial component was negligible.

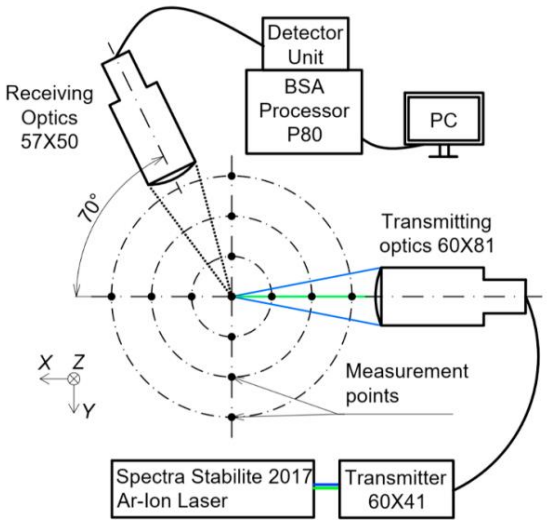

Fig. 5. Setup of the PDA measurement with a coordinate system [4]

Parameter	Value	
Laser power output	0.35 W	
Scattering angle	72°	
Receiver mask	C	
Receiver spatial filter	0.2 mm	
The focal length of transmitting/receiving optics	500/500 mm	
Wavelength	488 nm	514.5 nm
Velocity component	**Axial**	**Radial**
Velocity centre	25.7 m/s	0 m/s
Velocity span	51.4 m/s	24.4 m/s
Sensitivity	950 V	1080 V
SNR	0 dB	0 dB
Signal gain	8 dB	10 dB
Level validation ratio	8	8

Fig. 6. The main system parameters

The spray was probed at axial distances of Z = 100 mm from the exit orifice along two radially orthogonal axes. Measurements were taken between -27 and 27 at a 3 mm step between two adjacent points. In each measurement point, either 20 000 samples were acquired, or a 12 second acquisition duration was achieved, whichever required the shorter time interval.

The PDA measurement was controlled by the Dantec BSA software 5.2.

For ID_{32} the standard equation was used [1]:

$$ISMD = ID_{32} = \left(\sum_{i=1}^{n} r_i f_i D_{30,i}^3\right) / \left(\sum_{i=1}^{n} r_i f_i D_{20,i}^2\right) \quad (1)$$

where r_i is a radial distance from the spray centreline, f_i is the data-rate, D_{20} is a surface mean diameter and D_{30} is a volume mean diameter.

For *SCA* was used a simplified equation [4]:

$$SCA = 2 \cdot arctg\left(\frac{\frac{90 - Q_{cumulative_{n+1}}}{\frac{\left(Q_{cumulative_n} - Q_{cumulative_{n+1}}\right)}{(p_{n+1} - p_n)}} + p_{n+1}}{z}\right) \cdot 180 \cdot \pi \quad (2)$$

where *z* is the height coordinate.

The equation for C_d:

$$C_d = \frac{Q_{liquid}}{\frac{\pi \cdot d_{exit\_orifice}^2}{4} \cdot \sqrt{2 \cdot \rho_{liquid} \cdot p_{liquid}}} \quad (3)$$

3 Results and discussion

All selected parameters were considered in relation to *GLR*, as it corresponds to the energy operational requirements.

The first discussed parameter is ID_{32}, see Fig. 7 and Fig. 8, as it provides the global representation of the Sauter mean diameter by its mass-weighted averaging over the entire radial profile [3].

The CF1 atomizer produced a spray with lower ID32 compared to CF2 at both operating pressures, see Fig. 7. and Fig. 8. This can be attributed to the flow characteristic in the mixing chamber, which is related to the pressure difference and velocity profile. For all investigated CF1 modes, it can be assumed that the expansion occurs downstream of the exit orifice, since the pressure inside the mixing chamber was identical to the air pressure. For CF2, the expansion ratios varied, reflecting pressure drops of 0.167, 0.29 and 0.592 on average for all outlet diameters, in order. In all cases, the pressure difference grew in proportion to the growth of GLR. It can be concluded that, as the exit orifice increases, more expansion occurs in the mixing chamber.

An approximate relationship reflecting ID_{32} versus *GLR* and the exit orifice was obtained in the following form.

$$ID_{32} = 143 \cdot GLR^{-0.35} \cdot D_{exit\_orifice}^{0.3} \qquad (4)$$

The magnitude of ID_{32} has a decreasing trend with increasing *GLR*. The highest ID_{32} of about 140 µm was obtained at 100 kPa pressure, *GLR* 5 for the CF2 atomizer. The lowest values below ID_{32} of 60 µm were obtained for *GLR*, around 200 kPa pressure and CF1 nozzle with 1.0- and 1.5-mm exit orifice diameter.

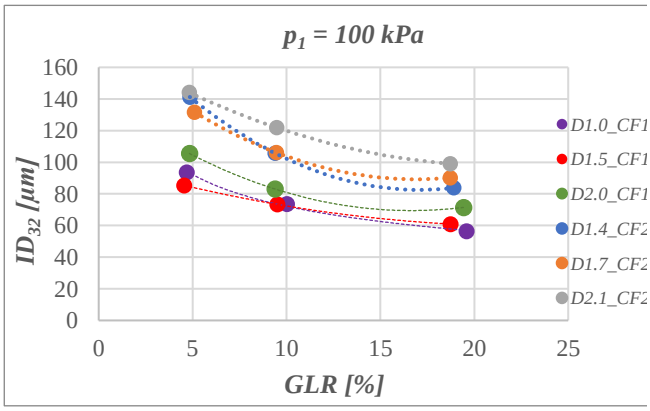

Fig. 7. The influence of *GLR* on ID_{32} for p_1 = 100 kPa

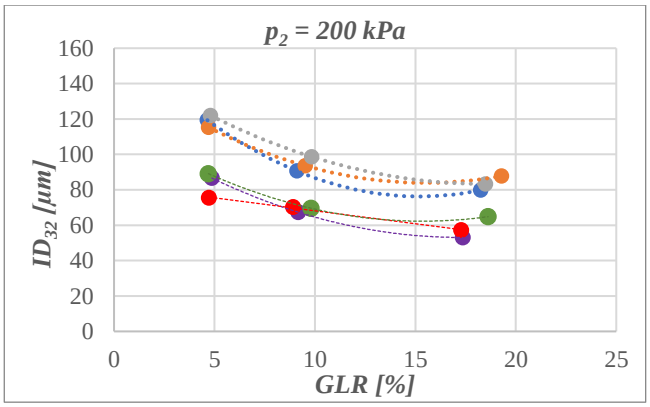

Fig. 8. The influence of *GLR* on ID_{32} for p_2 = 200 kPa

In general, it was expected an increase in *SCA* with *GLR* for two-fluid atomizers [5]. Looking at Fig. 9 for p_1, this only occurs for the D1.5_CF1 and D1.0 CF1 atomizers, where a slight downward trend for D2.0_CF1 can be seen. For all the CF2 atomizers, a convex trend can be observed. For p_2 (Fig. 10), a larger SCA appears but the trends of the *SCA* are similar to those of p_1 = 100 kPa.

In order to find a definite cause for this trend, it is necessary to test several modes and investigate the potential changes in the internal flow.

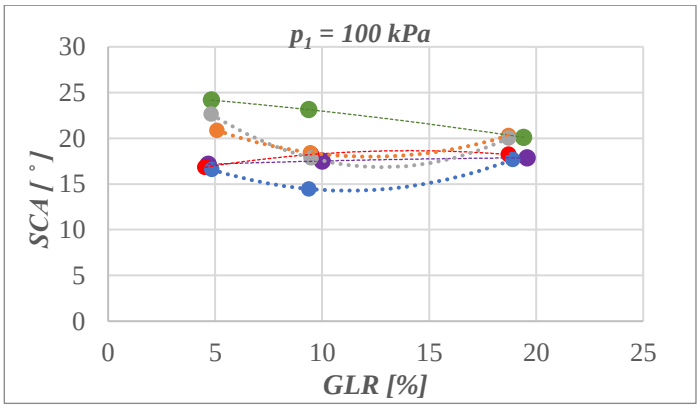

Fig. 9. The influence of *GLR* on *SCA* for p_1 = 100 kPa

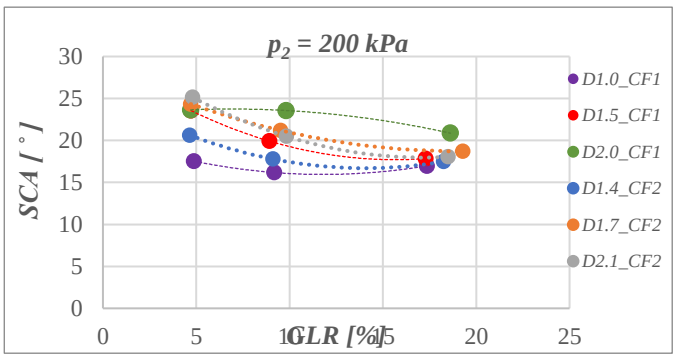

Fig. 10. The influence of *GLR* on *SCA* for p_2 = 100 kPa

C_d is decreasing with *GLR* increase for all tested variants, see Fig. 11. and **Chyba! Nenalezen zdroj odkazů.**. This is typical for twin-fluid atomizers. The lowest C_d values are obtained for atomizer D1.5_CF1, the

highest for D1.4_CF2. The CF2 exhibits a systematically higher C_d compared to CF1. The increasing exit orifice diameter tends to reduce the C_d values, which is comparable with effervescent atomizers where C_d increases with decreasing GLR and also with decreasing exit orifice [6].

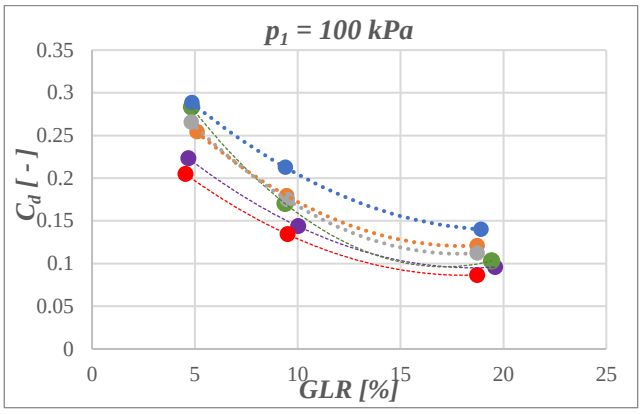

Fig. 11. The influence of *GLR* on C_d for p_1 = 100 kPa

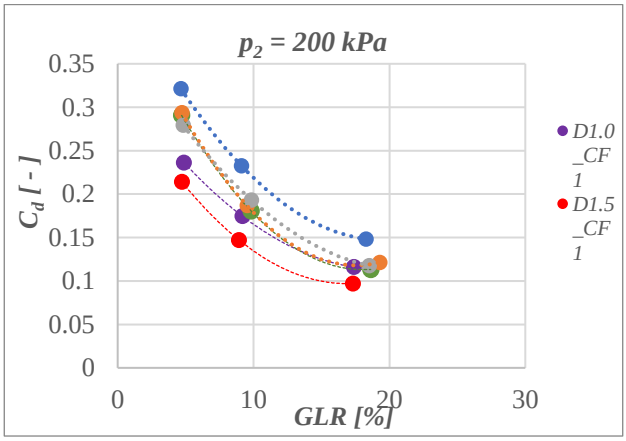

Fig. 12. The influence of *GLR* on *SCA* for p_2 = 100 kPa

4 Conclusion

In this study, the hypothesis of a significant effect of internal expansions on the performance of the atomizer was confirmed. The CF1 atomizer was observed to have a lower internal expansion rate and thus it behaved more as expected for a conventional twin-fluid atomizer.

The ID_{32} for both types of atomizers increased as the orifice dimeter increased and the *GLR* decreased. Larger droplets were obtained for CF2. This was observed for both operating pressures.

For *SCA*, we observed the strongest effect of the ratio of external to internal expansion. The *SCA* shown an increasing trend only partially for CF1 which has the expansion mostly occurring downstream of the exit orifice. The CF2 atomizers performed a rather convex trend. C_d increased with decreasing *GLR* and increasing pressure.

Highspeed imagining would be useful for further investigation, as it appeared that, due to the long counterflow channel in CF2, the expanding air localized the liquid to the centre, forming a narrow spray cone and affecting the Cd progression.

In future research, there is a necessity to further investigate the effect the counterflow canal. Also, the internal flow should be studied to explain the mixing process inside the atomizer for different expansion rates.

Acknowledgement

This work was supported by the Ministry of Education, Youth and Sports of the Czech Republic under the project LTAIN19044 funded from the program INTER EXCELLENCE (INTER–ACTION).

References

1. A. Hoxie, E. Johnson, V. Srinivasan, P. Strykowski, *ICLASS*, ***14***, *(*2018)
2. R. Rangarajan, H. Zhang, P. L. Strykowski, A. Hoxie, S. Yang, V. Srinivasan, *Com., Fu. And Em.*, ***4B***, *(2020)*
3. J. Jedelsky, M. Jicha, *Applied Energy*, **132(C)**, (2014)
4. M. Maly, M. Sapik, O. Cejpek, G. Wigley, J. Katolicky, J. Jedelsky, *Experimental Thermal and Fluid Science*, **106**, (2019)
5. A. H. Lefebvre, V. G. Mcdonell. Atomization and Sprays, **2**, (2017)
6. M. Ochowiak, L. Broniarz-press, J. Rozanski, *Experimental Thermal and Fluid Science*, **34(8)**, (2010)

Appendix B

```python
#calculation of the drag coefficient
def c_d(v_p, nu = 15.11e-6, d = 0.2):
# v_p - counterflow [m/s]
# nu - kinematic viscosity [N*s/m2]
# d - characteristic dimension of the measuring section [m]
    reynoldsNum = v_p * d / nu

    if reynoldsNum < 1:
        c_d = reynoldsNum*(24/reynoldsNum + 3/np.sqrt(reynoldsNum) + 0.34) + (1 - reynoldsNum)*(24/reynoldsNum)
    elif reynoldsNum < 2000:
        c_d = 24/reynoldsNum + 3/np.sqrt(reynoldsNum) + 0.34
    else:
        c_d = 10000/reynoldsNum*(24/reynoldsNum + 3/np.sqrt(reynoldsNum) +0.34) + (1 - 10000/reynoldsNum)*0.445
    return c_d
```

[15] ✓ 0.8s

```python
# import of libraries
import numpy as np
import matplotlib.pyplot as plt
from scipy.integrate import odeint  # import of function for numerical solution of ODE
from scipy.integrate import cumulative_trapezoid # import of function for numerical integration
from scipy.constants import g
```

[17] ✓ 0.9s

```python
def quadratic(v_z, t, kappa, v_p):

    dvdt = np.sign(v_p - v_z) * kappa * (v_z - v_p)**2
    return dvdt

def quadratic_cusatom_c_p(v_z, t, m_droplet, r_droplet, v_proud, gravity = False):

    rho_air = 1.225  # kg/m^3
    mu_air = 1.825e-5  # kg/ (m/s)
    rho_droplet = 997  # kg/m^3
    m_droplet = rho_droplet * 4 * np.pi * r_droplet**3
    S_droplet = np.pi * r_droplet**2
    k = 0.5 * rho_air * S_droplet* c_d(abs(v_z - v_proud))
    kappa = k/m_droplet
    if gravity:
        dvdt = np.sign(v_proud - v_z) * kappa * (v_z - v_proud)**2 + g
    else:
        dvdt = np.sign(v_proud - v_z) * kappa * (v_z - v_proud)**2
    return dvdt
```

[18] ✓ 0.1s

```python
v_0 = 35  # droplet velocity when exiting the atomizer
alpha = np.deg2rad(25/2)  # elevation angle from the z-axis
t = np.linspace(0, 0.2, 20000) # time points for numerical integration (start, end, number of steps)
v_p = -5 # counterflow speed
r_droplet = 10e-6  # m, radius od the droplet

v_r0 = np.sin(alpha)*v_0
v_z0 = v_0 * np.cos(alpha)

rho_air = 1.225  # kg/m^3
mu_air = 1.825e-5  # kg/ (m/s)

rho_droplet = 997  # kg/m^3

m_droplet = rho_droplet * 4 * np.pi * r_droplet**3
S_droplet = np.pi * r_droplet**2

k = 0.5 * rho_air * S_droplet* c_d(v_p)
kappa = k/m_droplet

# solve ODEs
v_z = odeint(quadratic_cusatom_c_p, v_z0, t, args=(m_droplet, r_droplet, v_p))[:, 0]
v_z_corected = odeint(quadratic_cusatom_c_p, v_z0, t, args=(m_droplet, r_droplet, v_p, True))[:, 0]
v_r = odeint(quadratic_cusatom_c_p, v_r0, t, args=(m_droplet, r_droplet, 0))[:, 0]
# path calculation by numerical integration
z = cumulative_trapezoid(v_z, t)
z_corected = cumulative_trapezoid(v_z_corected, t)
r = cumulative_trapezoid(v_r, t)

plt.figure(dpi=300)
plt.plot(z, r, label = 'Gravity neglected')
plt.plot(z_corected, r, label = 'Gravity used')
plt.gca().set_aspect(1.0)  # sets the ratio of axes in the plot
plt.xlabel('z (m)')
plt.ylabel('r (m)')
plt.grid()
plt.legend()
```

[20] ✓ 0.4s